Facilitatory stimulation of the pre-SMA in healthy aging has distinct effects on task-based activity and connectivity

Sandra Martin[1,2] ✉**, Regine Frieling**[1]**, Dorothee Saur**[2]**, and Gesa Hartwigsen**[1]

[1]Lise Meitner Research Group Cognition and Plasticity, Max Planck Institute for Human Cognitive and Brain Sciences, Leipzig, Germany; [2]Language & Aphasia Laboratory, Department of Neurology, University of Leipzig Medical Center, Leipzig, Germany

Semantic cognition is central to communication and our understanding of the world. It is usually well preserved in healthy aging. However, semantic control processes, which guide semantic access and retrieval, decline with age. The present study explored the potential of intermittent theta burst stimulation (iTBS) to enhance semantic cognition in healthy middle-aged to older adults. Using an individualized stimulation approach, we applied iTBS to the pre-supplementary motor area (pre-SMA) and assessed task-specific effects on semantic judgments in functional neuroimaging. We found increased activation after effective relative to sham stimulation only for the semantic task in visual and dorsal attention networks. Further, iTBS increased functional connectivity in domain-general executive networks. Notably, stimulation-induced changes in activation and connectivity related differently to behavior: While increased activation of the parietal dorsal attention network was linked to poorer semantic performance, its enhanced coupling with the pre-SMA was associated with more efficient semantic processing. Our findings indicate differential effects of iTBS on activity and connectivity. We show that iTBS modulates networks in a task-dependent manner and generates remote network effects. Stimulating the pre-SMA was linked to more efficient but not better performance, indicating a role in domain-general semantic control processes distinct to domain-specific semantic control.

TMS | TBS | fMRI | Semantic cognition | Language

Correspondence: *Sandra Martin* `martin@cbs.mpg.de`

Word count:

Abstract: 199 words
Main text: 4993 words

Introduction

Aging is accompanied by a myriad of cognitive changes. While the decline of executive functions, such as working memory, attention, and inhibitory control, and episodic memory are hallmarks of cognitive aging (Hedden and Gabrieli, 2004), functions that rely on the acquired knowledge about the world (semantic memory), such as language and creativity, usually remain well preserved and are affected by more subtle changes in healthy aging, for example increasing word retrieval problems (Henderson and Wright, 2016; Verhaeghen, 2003; Burke and Shafto, 2004). Moreover, increasing age has been associated with difficulties in language comprehension on the sentence and discourse level when processing becomes cognitively demanding, for instance through length, complexity, or ambiguity (Goral et al., 2011; Kemper et al., 2004; Obler et al., 1991). In light of the intact semantic knowledge system in healthy older adults, these changes have been attributed to declining cognitive control functions, which contribute to successful semantic processing when, for example, ambiguities need to be resolved or irrelevant information needs to be inhibited (DeDe and Knilans, 2016). In line with this notion, a recent study demonstrated an age-related decline of semantic selection processes, such as inhibiting irrelevant semantic associations, but not semantic representation and retrieval abilities (Hoffman, 2018). Notably, semantic selection was strongly correlated with non-semantic executive functions, underlining the role of domain-general cognitive control in semantic processing.

On the neural level, semantic cognition activates a mainly left-lateralized, widespread neural network in young adults, including frontal, temporal, and parietal regions (Binder et al., 2009; Jackson, 2021; Noonan et al., 2013). This network is thought to consist of distinct, yet interacting elements: a subnetwork for semantic representation and a subnetwork for semantic control (Lambon Ralph et al., 2017). Importantly, semantic control might be multidimensional as well, consisting of domain-specific semantic control, which subserves processes such as the controlled retrieval of less salient conceptual features, and domain-general control, which supports general selection and inhibition mechanisms (Hoffman, 2018). This notion is supported by the observation that brain regions that are active in tasks with high semantic control demands partially overlap with areas of the multiple-demand network (MDN), which refers to a set of frontoparietal brain regions involved in top-down cognitive control across domains (Duncan, 2010; Fedorenko et al., 2013).

In the aging brain, semantic cognition is characterized by a shift of the functional network architecture, which is reflected by increased activity of the MDN (for a review, see Hoffman and Morcom, 2018) and greater functional connectivity between domain-general networks such as the default mode network (DMN) and dorsal and ventral attention networks during semantic processing (Martin et al., 2022). This shift has also been described as reduced specialization of "core" processing areas of a task and increased neural dedifferentiation (Grady, 2012; Park et al., 2004). The behavioral relevance of these neural changes remains a point of debate. While the best preservation of cognitive functions has been associated with a youth-like pattern (Cabeza et al., 2018; Grady, 2012; Spreng et al., 2010), some changes might represent unsuccessful or attempted compensation (Hoffman and Morcom, 2018) whereas other reorganization processes have been linked to preserved, albeit less efficient semantic processing (Martin et al., 2022).

Non-invasive brain stimulation (NIBS) techniques are recognized as a promising approach to counteract age-related cognitive decline and to promote successful aging. Similar to the use of NIBS to boost neuropsychological rehabilitation after disruption of function due to stroke, these techniques might have the potential to support preservation of cognitive functions in pathological but also healthy aging through modulation of cortical excitability and the enhancement of neuroplasticity (Hartwigsen, 2018, 2015; Siebner et al., 2009). While there are some first promising results from different cognitive domains (for reviews, see Booth et al., 2022; Goldthorpe et al., 2020; Hsu et al., 2015), particularly when NIBS is coupled with training interventions, variability remains high and some studies find no beneficial effect of stimulation (e.g., Antonenko et al., 2022). Further insight into the potential of NIBS in aging can be gained by investigating the effect of stimulation on neural activity and functional connectivity. Neuroimaging results can help interpreting behavioral effects and might even be observed in the absence of a stimulation-induced behavioral change (Abellaneda-Pérez et al., 2022). In the domain of semantic cognition, only a few studies explored the effect of electrical stimulation at the neural level. These studies associated improved performance with a reduction of age-related upregulation in activity (Holland et al., 2011; Meinzer et al., 2013) and increases in functional connectivity between task-relevant regions of interest in the prefrontal cortex (Holland et al., 2016). So far, no study explored the potential of transcranial magnetic stimulation (TMS) to modulate age-related changes in semantic cognition on the behavioral and neural level.

Some studies investigated the potential of patterned repetitive transcranial magnetic stimulation to enhance performance in different cognitive tasks in healthy young brains (for a review, see Demeter, 2016). These studies report improved task performance after intermittent theta burst stimulation (iTBS; Huang et al., 2005). Fewer studies explored the modulatory effects of TBS on cognition in aging brains (Debarnot et al., 2015; Legon et al., 2016; Vidal-Piñeiro et al., 2014; Hermiller et al., 2022). The results of these studies are heterogeneous, and only one study found improved memory performance after iTBS (Debarnot et al., 2015), whereas others revealed changes in task-related activity and connectivity only (Vidal-Piñeiro et al., 2014) or non-specific effects of inhibitory stimulation (Hermiller et al., 2022). A better understanding of the modulatory effects of TBS at the neural level may help to increase the efficiency of network stimulation in aging brains. Moreover, such network approaches may be more powerful than conventional modulatory applications that target specific brain regions within specialized networks (e.g., Hartwigsen and Volz, 2021).

The goal of the present study was to explore the potential of iTBS to enhance semantic cognition in healthy middle-aged to older adults. We applied effective and sham iTBS to the pre-supplementary motor area (pre-SMA) and subsequently assessed the effect of stimulation using task-based functional magnetic resonance imaging (fMRI). The pre-SMA was selected as target area since it has been associated with the semantic control network and the domain-general MDN (Fedorenko et al., 2013; Jackson, 2021) emphasizing its role in mediating cognitive control across domains. Moreover, the pre-SMA contributes more to semantic processing in older relative to young adults (Martin et al., 2022) and represents a hub region in task-related functional networks of older adults, facilitating integrative processing (Martin et al., 2022). Using a semantic judgment task with varying cognitive demands and a tone judgment task as non-verbal control task, we hypothesized that iTBS might show stronger effects on the more demanding semantic condition. Further, comparing the effects of the tone with the semantic judgment task, allowed us disentangling task-specific effects of iTBS from general effects on control processes. Finally, we aimed to elucidate how stimulation-induced changes in task-related activity and functional connectivity relate to behavioral modulation.

Results

We implemented a single-blind, cross-over study design with three task-based functional magnetic resonance imaging (fMRI) sessions per participant (14 female; M = 61.6, SD = 7.64, range: 45–74 years; Figure 1A). During each session, participants completed a semantic judgment task and a tone judgment task (Figure 1B & C). Using the fMRI data from the first session, we applied an individualized stimulation approach where the stimulation coordinates of each participant were based on activation patterns within a pre-defined mask of the pre-supplementary motor area (pre-SMA; Ruan et al., 2018). During the second and third session, partici-
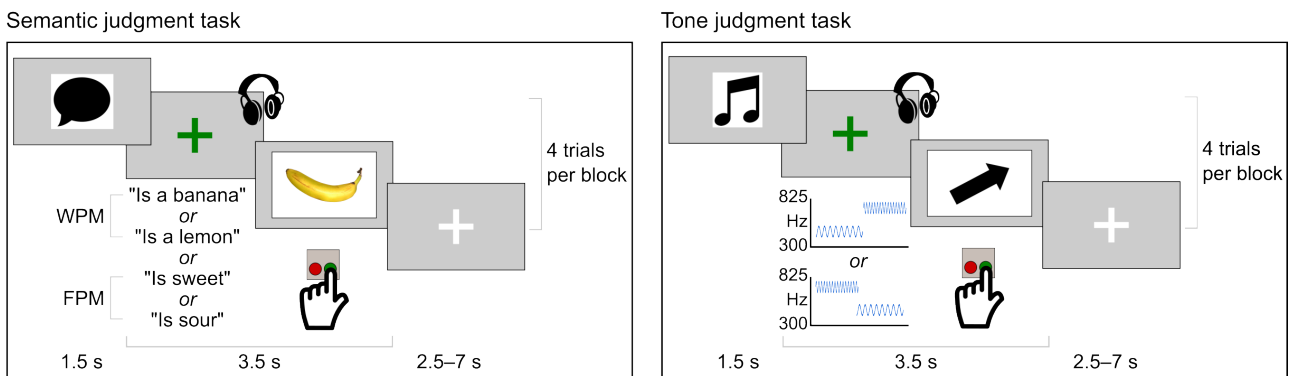
A Experimental design
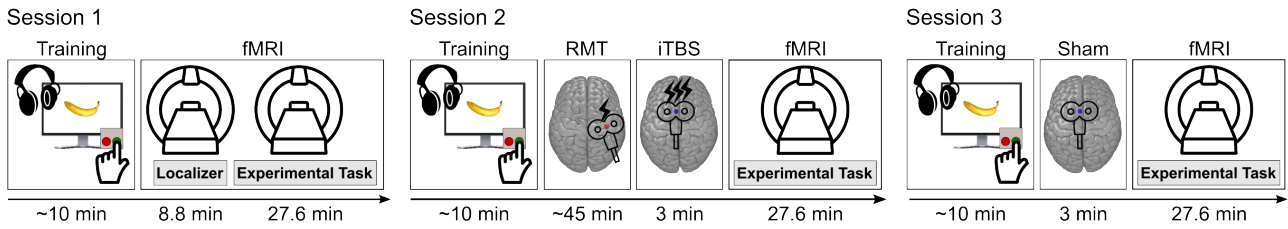
B Experimental paradigm
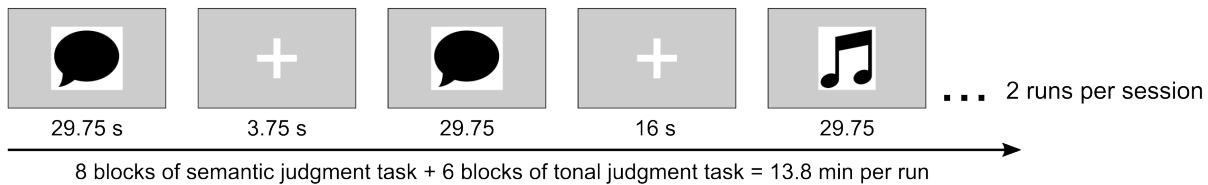
C Example trial of each task

Figure 1. Experimental Design. (A) Participants completed three sessions: a baseline fMRI session and two iTBS + fMRI sessions with effective and sham stimulation. (B) Per fMRI session, two task runs were completed. Blocks of the semantic judgment and the tone judgment task were interspersed with rest blocks. (C) Example trials for the semantic and the tone judgment task are shown. Participants heard a short phrase or a sequence of two tones. At the offset of the auditory stimulus, a picture of an object or an arrow appeared. Participants indicated via button press whether auditory and visual stimuli matched. RMT: resting motor threshold, WPM: word-picture matching, FPM: feature-picture matching.

pants then received once effective and once sham iTBS over the pre-SMA prior to fMRI (Figure 1A).

Behavioral results

We were interested in potential effects of iTBS on behavioral performance (Figure 2A and B). To this end, we fitted mixed-effects models for accuracy and reaction time data of the in-scanner tasks of word-picture, feature-picture, and tone-picture matching. For accuracy, the three-way interaction between session, condition, and congruency was not significant (x^2 = 7.83, p = 0.099). However, we detected a significant interaction between condition and congruency (x^2 = 53.15, p < 0.001) and session and condition (x^2 = 21.8, p < 0.001; Figure 2C). Post-hoc tests showed that incongruent items had higher accuracy in all conditions. However, the difference between congruent and incongruent items was only significant for word-picture matching (WPM; OR = 0.38, p < 0.001) and feature-picture matching (FPM; OR = 0.31, p < 0.001). For session

and condition, post-hoc tests showed a significant difference in accuracy only for the tone judgment task, such that participants performed generally better after the baseline session (active iTBS > baseline: OR = 0.41, p < 0.001; sham iTBS > baseline: OR = 0.57, p = 0.002). Moreover, we found main effects of condition (x^2 = 279.34, p < 0.001) and congruency (x^2 = 77.32, p < 0.001) but not of session (x^2 = 2.79, p = 0.25). Post-hoc tests revealed generally better performance for word-picture than feature-picture matching (OR = 5.77, p < 0.001) and the tone-picture matching condition (OR = 3.55, p < 0.001; Figure 2C). For congruency, accuracy was higher for incongruent than congruent items (OR = 0.5, p < 0.001).

For reaction time, results showed a significant interaction of session with condition (x^2 = 44.4, p < 0.001; Figure 2D). Post-hoc tests revealed that reaction times improved for all three conditions after the baseline session (all p < 0.01). However, there was no difference in reaction time between effective and sham iTBS ses-
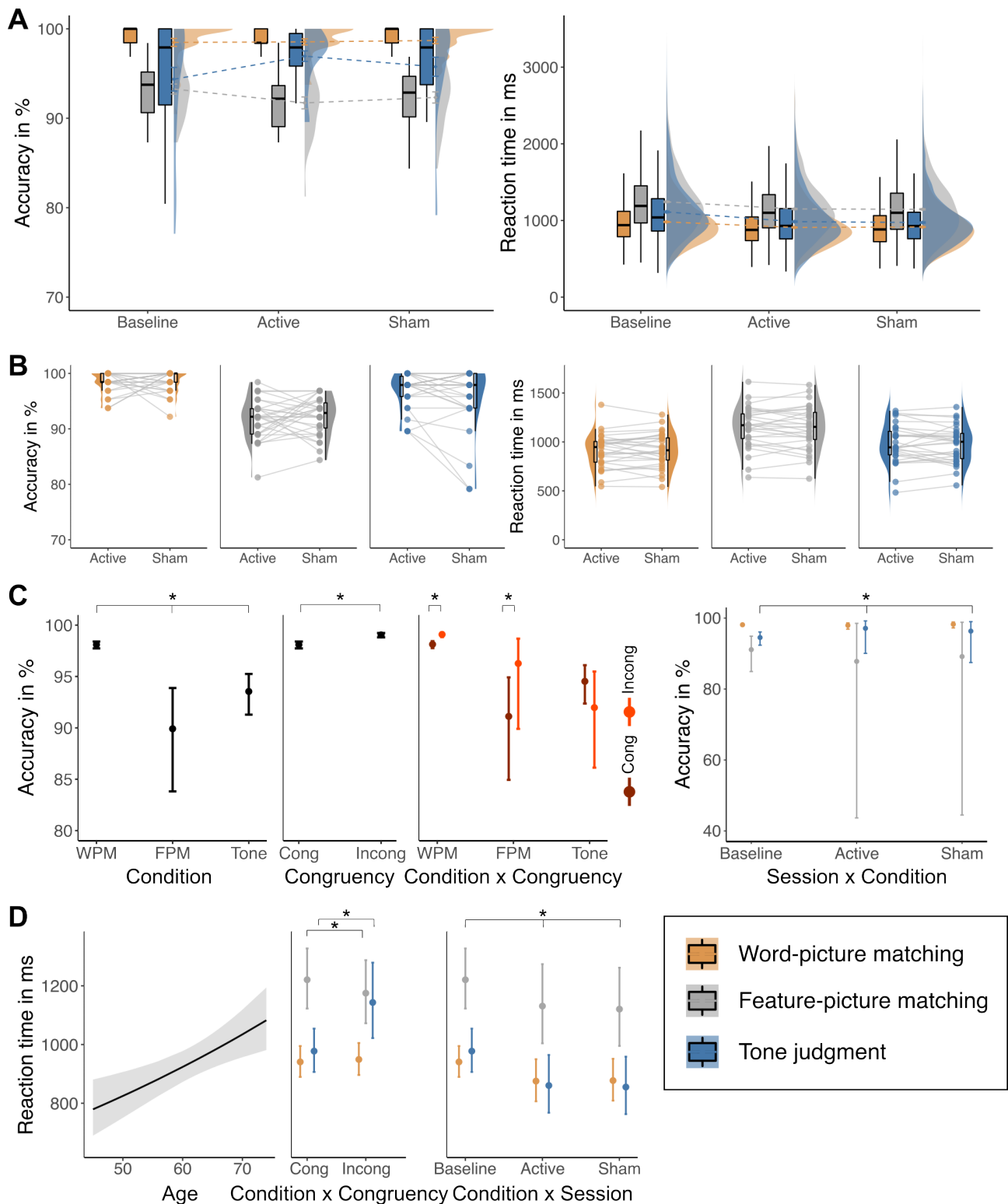
Figure 2. Behavioral results. (A) Results for accuracy and reaction time for each condition at each session. Boxplots show median and 1.5 x interquartile ranges. Half-violin plots display distribution and dotted lines show changes of mean values across sessions. (B) Individual data for effect of stimulation sessions on accuracy and reaction time for each condition. (C) and (D) display significant results of mixed-effects regression for accuracy and reaction time. Cong: congruent items, Incong: incongruent items.

sions. Results also showed a significant interaction between condition and congruency (x^2= 306.53, p < 0.001). Post-hoc comparisons revealed that for FPM, incongruent items were faster (p = 0.034), while for tone-picture matching, congruent items were faster (p < 0.001). Further, we found a significant effect of age on reaction time with reaction times generally increasing with age (x^2= 9.4, p = 0.002). Full results of both models are shown in Table S4.

Univariate functional MRI data

The effect of conditions at baseline

For the semantic judgment task, we found a large left-lateralized fronto-temporo-parieto-occipital network with additional activation in the right hemisphere (Figure 3A; Table S5). An additional cluster spanned the pre-SMA. The control task of tone judgment revealed a bilateral network with clusters in frontal, temporal, parietal, and occipital regions (Figure 3A; Table S5). We were interested in the difference in brain activation between the semantic judgment and the tone judgment task. The contrast semantic judgment > tone judgment activated a mainly left-lateralized fronto-temporal network for semantic processing encompassing left inferior frontal gyrus, left anterior, middle, and superior temporal gyri, and bilateral fusiform gyri (Figure 3B; Table S5). Further, precuneus, superior frontal gyrus, and frontal pole were activated. The opposite contrast, tone judgment > semantic judgment, activated a mainly right-lateralized network including the right frontal pole, middle frontal gyrus, precuneus, and the right angular gyrus. Moreover, we found small clusters in left superior frontal gyrus and left inferior frontal lobe (Figure 3B; Table S5).

We also investigated the effect of semantic processing demand by comparing both conditions within the semantic judgment task with each other. For WPM, stronger activation in bilateral superior temporal gyri was detected when compared with FPM (Table S5). For the opposite contrast, FPM > WPM, results showed stronger activity in a left-lateralized network including inferior frontal gyrus, middle temporal gyrus, inferior parietal lobe, and superior frontal gyrus with supplementary motor area.

iTBS increases task-specific activity for semantic judgments in distributed networks

To explore the effect of iTBS and potential interactions with conditions, we contrasted effective and sham stimulation sessions. Results only revealed stronger activation after effective compared with sham sessions and only for the semantic judgment task. For semantic judgment > rest, we found stronger activation in the right posterior angular gyrus, superior temporal gyrus, middle occipital gyrus, and a cluster in left superior parietal lobe (SPL) and bilateral cuneus (Figure 4A; Table 1). This was mirrored by effects for the individual conditions of semantic judgment, WPM and FPM. For both

conditions, a cluster spanning left SPL and right cuneus was found (Table 1). Further, for FPM, an additional cluster in right angular gyrus as well as occipital and fusiform gyrus was detected. For the contrast semantic judgment > tone judgment, results showed a significant cluster in bilateral lingual gyri and left middle occipital gyrus (Figure 4B; Table 1).

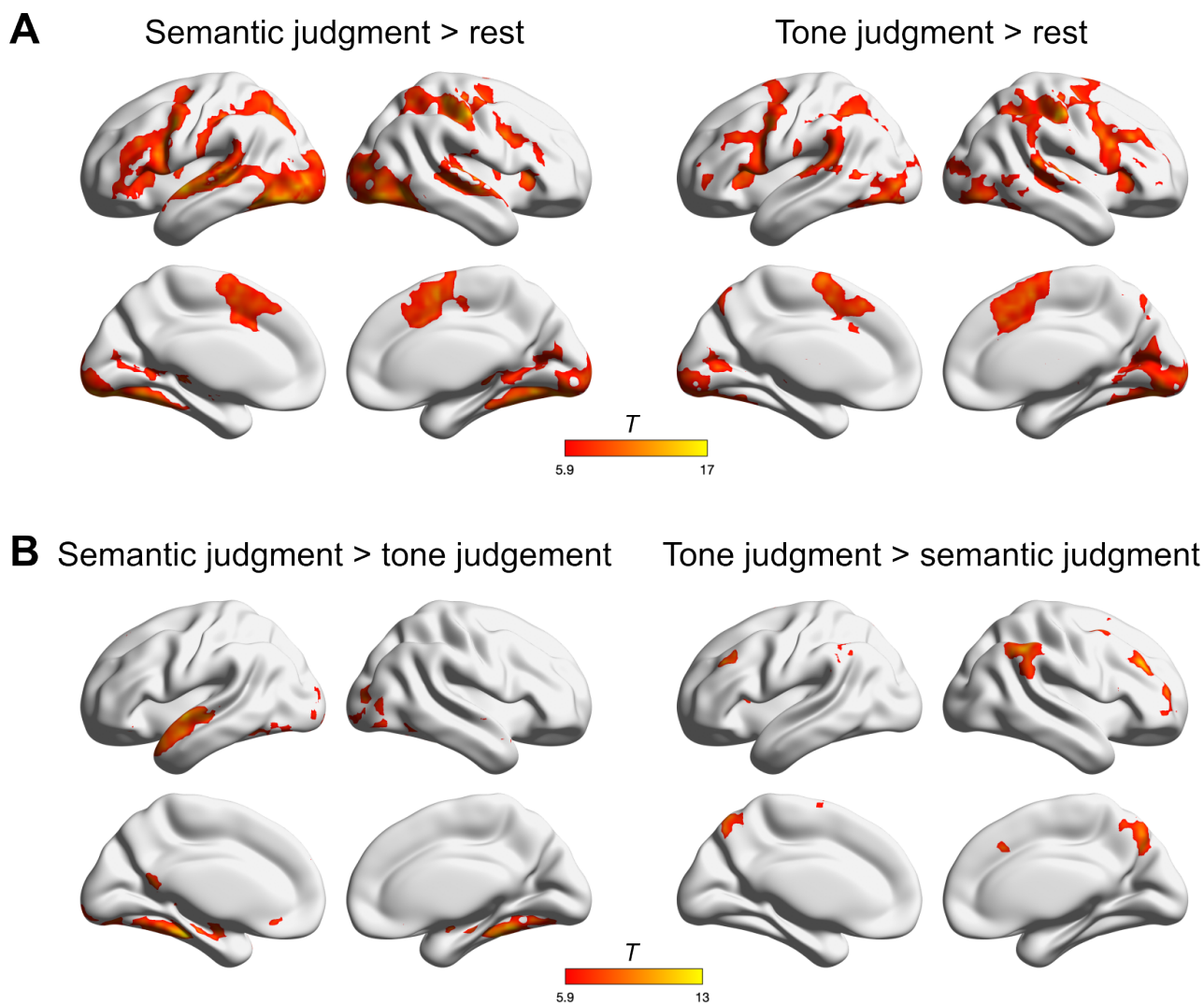#### Increased activity after iTBS is associated with poorer semantic performance

We correlated the difference in percent signal change (PSC; effective > sham iTBS) for the stimulation site pre-SMA and for cluster peaks that showed an effect of stimulation (n = 6; Table 1) with the difference in behavior. For the pre-SMA, we found that accuracy for the tone judgment task was negatively correlated with PSC (r = -0.36, p = 0.05) such that smaller PSC for effective relative to sham iTBS was associated with higher accuracy during the effective relative to the sham session (Figure 4C). Further, results showed a negative correlation for accuracy of the semantic judgment task with a cluster in left dorsal SPL (r = -0.37, p = 0.047; Figure 4D) which had shown stronger activity for semantic judgment > rest after effective relative to sham iTBS. We found that less PSC for effective compared with sham iTBS was associated with higher accuracy for effective relative to sham iTBS. This effect was further specified through the FPM condition which showed the same pattern for the cluster in left ventral SPL (r = -0.37, p = 0.044; Figure 4E). We did not detect any significant correlations for reaction time.

The effect of iTBS on subject-specific functional regions of interest (ROIs) for language processing

We extracted PSC for effective and sham iTBS sessions in the 25 subject-specific functional ROIs that were defined using a group-constrained subject-specific parcellation approach. We were interested in an effect of iTBS on PSC of the different conditions. To this end, we fitted linear mixed-effects models with predictors for session and PSC. We did not find any significant interaction between functional ROIs and session. Supplementary Figures S4-6 show the individual PSC values for both stimulation sessions for each ROI.

Effects of iTBS on functional connectivity (generalized PPIs)

Based on the activation patterns from the comparison of effective and sham iTBS, we conducted generalized psychophysiological interaction (gPPI) analyses for the significant cluster peaks. We asked whether and how effective iTBS generates changes in functional connectivity for these task-specific regions. Moreover, we were interested in a relationship between stimulation-induced changes in functional connectivity and behavior and assessed such associations for the PPI connectivity between the pre-SMA and significant cluster peaks from univariate results.

A

Semantic judgment > rest

Tone judgment > rest

B

Semantic judgment > tone judgement

Tone judgment > semantic judgment

Figure 3. Univariate activation results for experimental conditions during baseline session. (A) shows results for each experimental task against rest (implicit baseline) while (B) displays the results when both tasks are contrasted ahainst each other. Results are FWE-corrected at peak level p < 0.05 with a minimal cluster size k = 10 voxels.

### *iTBS reduces task-specific connectivity for parietal areas during semantic processing*

One-sample t-tests for the difference in functional connectivity between effective and sham stimulation revealed significant changes for three seed regions: the left dorsal and ventral SPL and the right cuneus. For all regions, we found reduced whole-brain connectivity after effective relative to sham iTBS for the contrast semantic judgment > tone judgment (Figure 5A; Table S6). The dorsal SPL showed reduced coupling with a cluster in the left middle frontal gyrus and frontal pole after effective stimulation. For the seed in the more ventral left SPL, we found a similar cluster in the frontal pole, which also extended into the anterior cingulate gyrus. Moreover, the ventral left SPL was negatively coupled with a cluster in the right superior frontal gyrus and pre-SMA, a region in the anterior left SPL, and the left precentral gyrus and superior frontal gyrus. The right cuneus showed greater decoupling with a cluster in the right frontal pole and middle frontal gyrus. To further

explore the interaction effect, we investigated the difference between effective and sham stimulation for the contrasts semantic judgment > rest and tone judgment > rest for the seed regions. Results showed that significant whole-brain decoupling for the cuneus was mainly driven by increased coupling of these regions during the tone judgment task (Figure S7). In the ventral SPL, a cluster in the left frontal pole was related to greater decoupling in the semantic and greater coupling in the control task after effective iTBS, thus dissociating both tasks (Figure S7).

Areas of decreased coupling belong to domain-general networks

We were interested in the representative networks of these stimulation-induced changes in functional connectivity. To this end, we plotted binary maps of the significant gPPI results together with a common seven-networks parcellation based on intrinsic functional connectivity (Yeo et al., 2011). Figure 5B shows the overlap
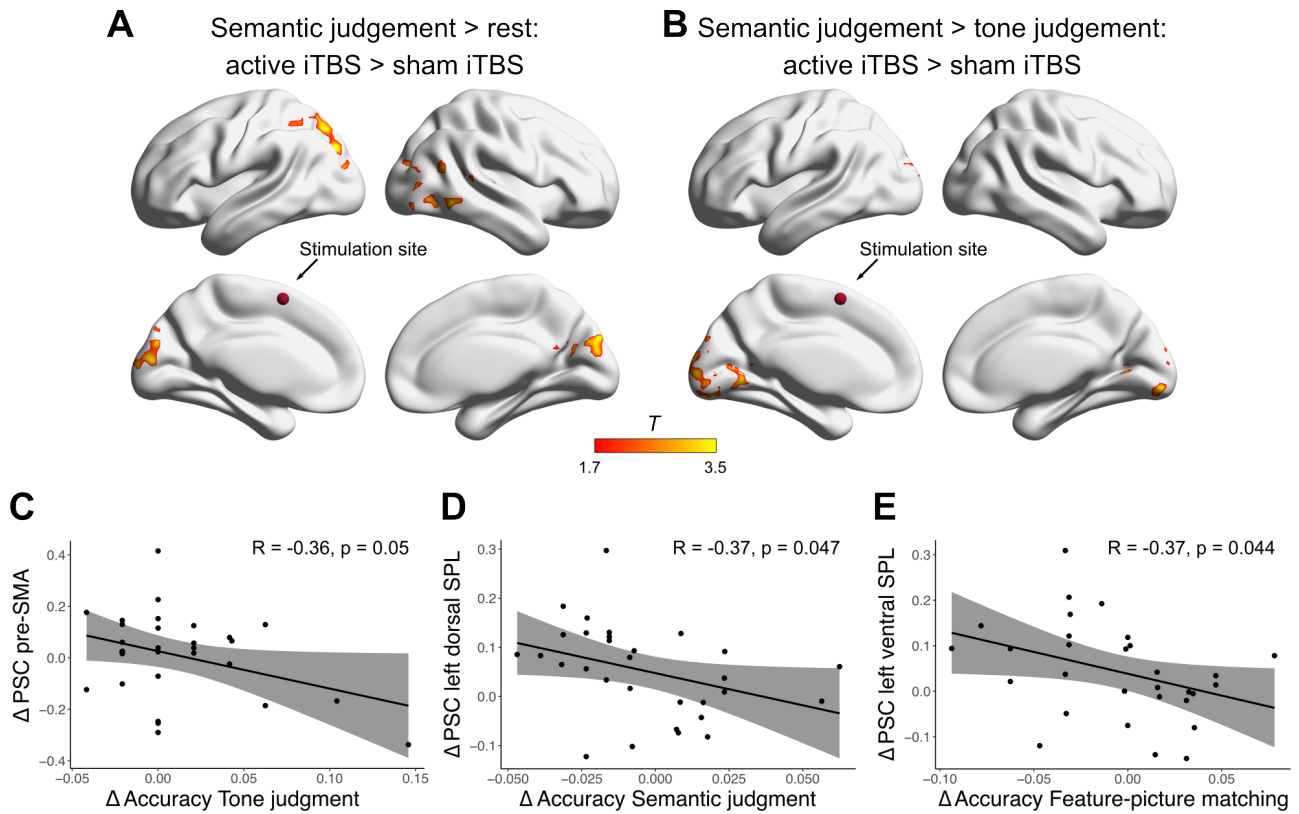
Figure 4. Effect of stimulation on brain activation. After effective stimulation, stronger activation was found for (A) semantic judgment > rest and for (B) semantic judgment > tone judgment. We then extracted percent signal change (PSC) for significant clusters and correlated the difference in PSC between effective and sham sessions with the difference in behavior between effective and sham sessions. (C) For Δ of accuracy of tone judgment, a negative correlation with the difference in PSC in our stimulation site pre-SMA was detected. (D) and (E): For Δ of accuracy of semantic judgment, and more specifically the FPM condition, a negative correlation with the difference in PSC in the left superior parietal lobe (SPL) was detected. fMRI results are thresholded at $p < 0.05$ at peak level and FWE-corrected at $p < 0.05$ at cluster level.

Table 1. Significant clusters for effective > sham iTBS

Anatomical structure	Hemisphere	k	t	x	y	z
Word-picture matching >Rest						
Cuneus	R	1387	3.87	9.52	-68.78	21.50
Superior parietal lobe	L		3.78	-22.82	-71.26	54.50
Superior occipital gyrus	R		3.59	21.96	-83.70	18.75
Feature-picture matching >Rest						
Angular gyrus, posterior division	R	672	4.11	54.30	-63.80	18.75
Middle occipital cortex	R		3.94	44.35	-83.70	7.75
Fusiform gyrus	R		3.36	29.42	-68.78	-6.00
Superior parietal lobe	L	763	3.45	-22.82	-71.26	46.25
Cuneus	L		3.43	-7.90	-86.19	40.75
Cuneus	R		3.32	7.03	-86.19	29.75
Semantic judgment >Rest						
Middle occipital gyrus	R	726	4.03	44.35	-81.22	7.75
Angular gyrus, posterior division	R		3.64	54.30	-63.80	18.75
Superior temporal gyrus	R		3.49	54.30	-28.97	5.00
Superior parietal lobe	L	959	3.86	-22.82	-71.26	54.50
Middle occipital gyrus	L		3.53	-25.31	-81.22	32.50
Superior parietal lobe	L		3.50	-22.82	-71.26	46.25
Semantic judgment >Tone judgment						
Lingual gyrus	L	1083	4.04	-17.85	-68.78	2.25
Middle occipital gyrus	L		3.78	-17.85	-91.17	18.75
Lingual gyrus	R		3.55	12.01	-71.26	2.25

Note. Results are thresholded at $p < 0.05$ at peak level and FWE-corrected at $p < 0.05$ at cluster level.

of the clusters that showed reduced coupling with the respective networks. Clusters in the frontal pole were associated with the DMN and in the middle frontal gyrus with the fronto-parietal control network. Furthermore, decoupled clusters from the ventral SPL were mainly linked to the ventral attention network, and in pre-central gyrus to the sensorimotor network.

Decreased coupling after iTBS is associated with slower semantic performance under effortful conditions

The change in functional connectivity between pre-SMA and left ventral SPL was associated with a change in behavior after effective stimulation (Figure 6). More specifically, a negative correlation (r = -0.49, p = 0.006) indicated that reactions for the FPM condition were slower the more those two regions were decoupled after effective iTBS.

Discussion

In light of global population aging and the associated increase in age-related diseases, new interventions are needed to counteract cognitive decline and promote successful aging. NIBS is increasingly recognized as a promising tool to boost cognitive functions in older adults. However, to design effective treatment protocols, a better understanding of the neural mechanisms of NIBS is mandatory. In particular, it remains unclear whether NIBS-induced improvements may be underpinned by decreases or increases in task-related activity and connectivity, or both. Here, we explored the effect of effective relative to sham iTBS over the pre-SMA on the behavioral and neural level during a semantic judgment task and a non-verbal control task. In the absence of direct stimulation-induced changes at the behavioral level, we found significant modulation of task-related activity and connectivity. These changes differed in their functional relevance at the behavioral level. Our main results were as follows: iTBS led to higher activation during semantic processing at remote regions in posterior areas (posterior temporal cortex, parietal, and occipital lobe). In contrast, functional connectivity results revealed reduced whole-brain connectivity of these upregulated areas during semantic processing, but increased connectivity for the tone judgment task. Strikingly, TMS-induced changes on activation and functional connectivity had differential effects on behavior. While upregulated regions were associated with poorer semantic performance, increasing connectivity between the stimulation site and a cluster in the dorsal attention network was linked to faster performance in the most demanding semantic condition. Overall, our findings indicate disparate effects of iTBS on activation and connectivity. Further, we show that iTBS modulates networks in a task-dependent manner and generates effects at regions remote to the stimulation site. Finally, our results shed new light on the role of the pre-SMA

in domain-general and semantic control processes, indicating that the pre-SMA supports executive aspects of semantic control.

Higher-order cognitive networks for semantic judgment and tone judgment that overlap in the pre-SMA

Our task paradigm revealed two widespread functional networks for semantic judgment and non-verbal tone judgment, which overlapped in sensory-motor systems for auditory, visual and motoric processing. We delineated specific networks by contrasting both tasks with each other. Semantic processing activated a left-lateralized fronto-temporal network, which aligns well with previous investigations and meta-analyses on semantic cognition (Binder et al., 2009; Jackson, 2021; Lambon Ralph et al., 2017). Notably, the network contained core areas of semantic representation, such as the bilateral temporal poles, but also semantic control, including the left inferior frontal gyrus and posterior middle temporal gyrus. Moreover, in contrast to the tone judgment task, semantic processing activated bilateral middle and posterior fusiform gyri. While the anterior fusiform gyrus (anterior temporal lobe) has been recognized as a key area of semantic processing (Chiou et al., 2018; Lambon Ralph et al., 2017; Mion et al., 2010), less work has focused on the role of the middle and posterior fusiform gyrus in semantic cognition. Although famous for the recognition of faces (Kanwisher et al., 1997), objects in general (Grill-Spector, 2003), and visual words (Dehaene and Cohen, 2011), a recent investigation on the spatiotemporal dynamics of semantic processing linked the middle fusiform gyrus to lexical semantics, thus suggesting a role behind early visual processes (Forseth et al., 2018). This notion aligns with our results which showed pronounced bilateral activation of this region compared with the tone judgment task.

Contrasting both conditions of semantic judgment, WPM and FPM, with each other, confirmed the intended modulation of cognitive demand: While WPM showed relative greater activation in left language perception areas, which points to a focus on phonological and lexical processing during this task, FPM activated core regions of semantic but also domain-general control, indicating increased task demand. The tone judgment task, on the other hand, activated a fronto-parietal network, which was based on regions of the frontoparietal control and the dorsal attention network. Notably, all the activated regions during tone judgment also fell within the MDN, confirming the non-verbal, high executive demand of this task.

iTBS does not produce direct behavioral changes at the group level

Although univariate fMRI results from the baseline session demonstrated the contribution of the pre-SMA to the semantic judgment and the non-verbal tone
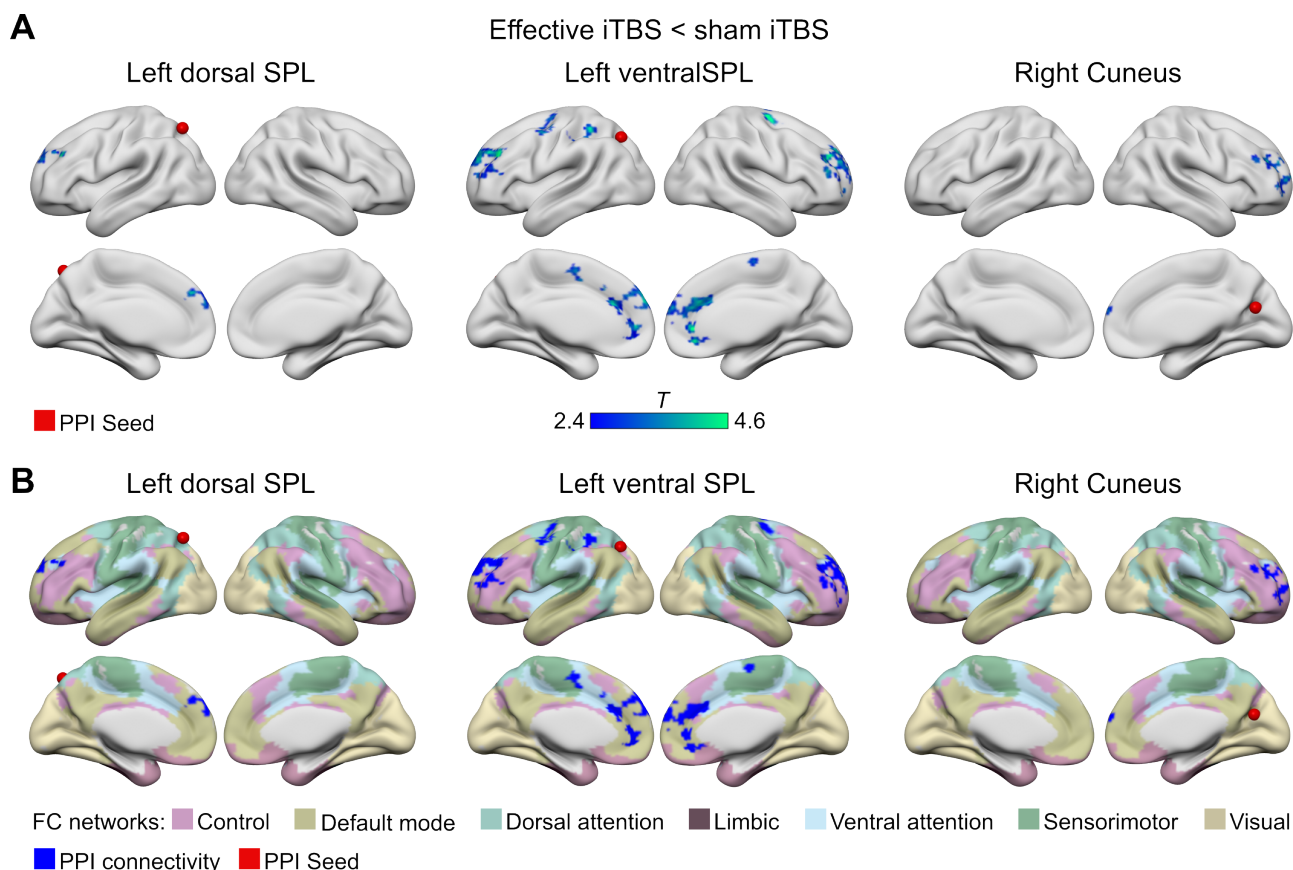
Figure 5. Functional connectivity results for cluster peaks that showed stronger activation after effective iTBS. (A) Three seeds showed stronger decoupling after effective relative to sham stimulation for the contrast semantic judgment > tone judgment. (B) Binary PPI activation maps plotted onto a seven-networks functional connectivity parcellation (Yeo et al., 2011). fMRI results are thresholded at p < 0.01 at peak level and FWE-corrected at p < 0.05 at cluster level.

judgment task, applying effective iTBS to the pre-SMA did not produce behavioral changes relative to the sham session. This result was unexpected. However, we are not the first study to observe stimulation-induced effects on the neural but not behavioral level in healthy older adults (Vidal-Piñeiro et al., 2014). The lack of a behavioral effect might be due to a number of reasons. First, in contrast to most studies, we included a separate baseline session, during which participants practiced and performed the tasks. This led to a notable improvement across all conditions, most strongly in the unfamiliar tone judgment task. Hence, familiarity with the paradigm after the baseline session might have aggravated the chance of observing a stimulation effect. This factor should be considered in future studies as well. Second, the effect of offline stimulation might not have been strong enough to induce behavioral changes. Although we took great care to minimize the time between end of stimulation and begin of task-based fMRI, this might have impeded the observation of a behavioral effect. Third, the applied tasks might have been too easy for our group of participants to observe a facilitatory effect of iTBS. This is the first study to use TBS in healthy aging in the domain of semantic cognition. While previous work successfully applied anodal transcranial direct current stimulation

to the left inferior frontal gyrus and motor cortex to enhance semantic word retrieval in healthy older adults (Holland et al., 2011; Meinzer et al., 2013, 2014), the facilitatory stimulation of an executive control hub that contributes to semantic control processes might not have been critical when task performance is already high. Nonetheless, though unintended, the absence of a stimulation effect on cognition allowed us to interpret alterations on the neural level without the confounds of behavioral changes that might make them harder to interpret otherwise (Blankenburg et al., 2010; Feredoes et al., 2011). Moreover, the behavioral relevance of these changes was demonstrated in the significant correlations between activity or connectivity increases and behavioral modulation.

iTBS over the pre-SMA increases activity in a widespread network of visual processing and cognitive control

Effective iTBS generated greater activity than sham iTBS in posterior regions but not at the stimulation site. This finding was surprising but is in line with the increasingly reported observation that TBS produces remote effects on activation in neural networks (Cárdenas-Morales et al., 2011; Halko et al., 2014; Vidal-Piñeiro
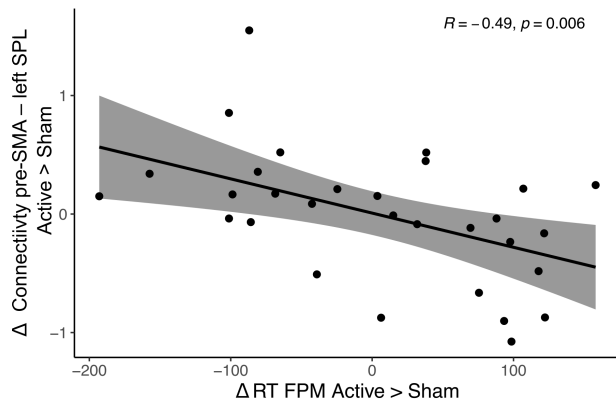
Figure 6. Relationship between stimulation-induced changes in functional connectivity and behavior. Reduced coupling of pre-SMA and left ventral SPL after effective iTBS was associated with slower reaction times (RT) during the feature-picture matching (FPM) condition.

et al., 2014). Notably, stimulation-induced changes in the BOLD signal were task-specific. Specifically, we found that activity only changed when participants were performing the semantic judgment task but not at rest or during the tone judgment task. For semantic judgments compared with the control task, increased activation was observed in the occipital cortex, including bilateral lingual gyri and medial occipital lobe, which indicates a specific role of these regions in the semantic but not the tone judgment task. This notion is supported by emerging evidence from healthy but also patient studies that the occipital cortex, particularly the lingual gyrus, supports language-related and verbal memory tasks (Amedi et al., 2004; Heath et al., 2012; Kim et al., 2011; Palejwala et al., 2021). Thus, the increased activation of these regions mediated by the pre-SMA might suggest a top-down control on visual processing regions in a task-specific manner. Moreover, comparing the semantic judgment task to rest revealed greater activation of clusters in left superior and right inferior parietal lobes apart from clusters in the occipital lobe after effective stimulation. These results were mainly driven by the FPM condition. All cluster peaks fell within the dorsal attention network, which illustrates a functional connection with focused attention, which is likely semantic-specific (Cristescu et al., 2006; Kim et al., 2011; Mahon and Caramazza, 2010).

iTBS decreases functional connectivity within cognitive control networks during semantic processing

We gained further insight into the role of the upregulated regions through functional connectivity analyses. Results showed reduced whole-brain functional connectivity for semantic judgments in dorsal and ventral SPL and the right cuneus after effective iTBS. The seeds in the left SPL showed strongest decoupling with a large prefrontal cluster in the left ventral attention network, while the cuneus was negatively coupled

with a prefrontal cluster in the right control network. Moreover, we found reduced connectivity of the ventral SPL with our stimulation site, the pre-SMA, the parietal dorsal attention network, and a cluster in the frontal pole associated with the DMN. Notably, apart from the cluster in the DMN, all cluster peaks fell within regions of the MDN. Moreover, the majority of significant clusters were driven by increased connectivity for the tone judgment task. This finding demonstrates the potential of iTBS to generate task-specific changes in functional network coupling, which is line with previous reports (Halko et al., 2014; Singh et al., 2020; Vidal-Piñeiro et al., 2014). Further, it suggests a TMS-induced modulation of whole-brain functional connectivity in response to executive and attention demands and supports the notion of the pre-SMA as an organizing hub in the MDN, coordinating the interaction of different cognitive control regions (Camilleri et al., 2018).

iTBS-induced changes in activation and functional connectivity relate differently to behavior

Relating TMS-induced changes on activation and functional connectivity with the cognitive performance allowed us to explore the behavioral relevance of these network changes (Figure 7). While it might seem surprising that the increased activation of the parietal dorsal attention network was linked to poorer accuracy in the semantic judgment task, this finding corroborates the notion that the most efficient task processing is associated with little or no additional functional activation apart from task-specific core regions. This is a common observation in neurocognitive aging, where increased activation and reduced deactivation of domain-general regions have been associated with neural inefficiency, leading to poorer performance across a range of cognitive domains (Cabeza et al., 2018; Spreng et al., 2010). Moreover, better and more efficient behavioral performance due to training-induced activation decreases has been reported in healthy participants (Abel et al., 2012; Horner and Henson, 2008) as well as post-stroke chronic aphasia (Abel et al., 2015; Richter et al., 2008). In our study, task performance was high and remained unchanged after iTBS, indicating a stimulation-induced upregulation of remote cognitive control regions that were not necessary for efficient task processing. Though speculative, a different pattern might have emerged through the perturbation of a domain-specific node in the semantic network. A recent study from our group found a partially compensatory upregulation of MDN regions when the domain-specific semantic network was disrupted (Hartwigsen et al., 2017).

Notably, increasing functional connectivity between our stimulation site and the upregulated cluster in the parietal dorsal attention network after iTBS was associated with faster reaction times in the most demanding semantic condition. This result strengthens the idea of a task-specific coupling of cognitive control regions

Facilitatory stimulation of a domain-general hub in semantic cognition
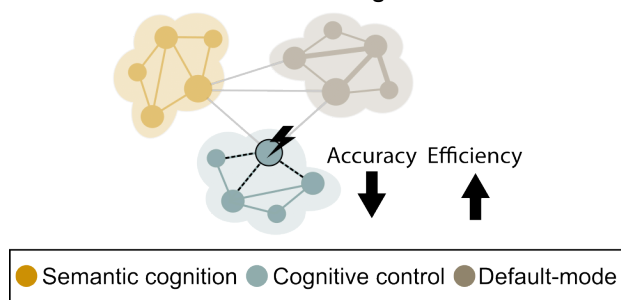
Figure 7. Facilitatory stimulation of a hub of the domain-general multiple-demand network enhanced coupling with other cognitive control networks distal to the stimulation site. This was linked to poorer performance but increased efficiency during semantic processing in a group of middle-aged to older adults.

that have been linked to executive components of semantic processing (Kim et al., 2011; Mahon and Caramazza, 2010) and language processing in general (Geranmayeh et al., 2014; Sliwinska et al., 2017). Here, we demonstrate that such coupling can enhance the processing efficiency when cognitive demands are high but not the cognitive process per se in form of improved accuracy.

In conclusion, our results agree with the proposal of an adaptive recruitment of domain-general resources to support language processing, which, however, are less efficient than the specialized domain-specific network (Hartwigsen, 2018). Moreover, we add a new perspective to the role of the MDN in semantic cognition: Our findings indicate that the pre-SMA supports semantic-specific processes through the upregulation of and coupling with cognitive control regions that have been linked to semantic cognition. Importantly, the pre-SMA did not upregulate or couple with regions of the domain-specific network of semantic control, such as the left inferior frontal gyrus and posterior middle temporal gyrus. Together with our findings of a positive effect of pre-SMA stimulation on task efficiency but not accuracy, we propose a multidimensionality of semantic control on the neural level beyond the inferior prefrontal cortex (Badre et al., 2005; Nagel et al., 2008), consisting of a fronto-temporal domain-specific and a fronto-parietal domain-general semantic control network. Stimulating the pre-SMA with facilitatory TMS modulated domain-general semantic control but had no effect on domain-specific control regions.

Limitations and outlook

It should be noted that we did not find an effect of stimulation on the subject-specific functional ROIs for language processing. Though unexpected, this aligns with our other results, indicating a modulation of domain-general and not language-specific regions through iTBS

over the pre-SMA. A future comparison of modulation of domain-general and domain-specific semantic control hubs could help to fully explore the contribution of both control systems to semantic cognition. Moreover, we cannot rule out the possibility that our results are limited to the aging brain. Although we tested a relatively wide range from middle to older age, future studies should consider a group of young participants for comparison.

Materials and Methods

Participants

A total of 30 healthy middle-aged to older adults (14 female; $M = 61.6$, $SD = 7.64$, range: 45–74 years) participated in the experiment. Inclusion criteria were native German speaker, right-handedness, normal hearing, normal or corrected-to-normal vision, no history of neurological or psychiatric conditions, and no contraindication to magnetic resonance imaging or rTMS. Participants were also screened for cognitive impairments using the Mini-Mental State Examination (Folstein et al., 1975; all $\geq 26/30$ points). Written informed consent was obtained from each participant prior to the experiment. The study was approved by the local ethics committee of the University of Leipzig and conducted in accordance with the Declaration of Helsinki.

Experimental Design

Figure 1 displays the experimental procedure. The study employed a single-blind, cross-over design with three sessions per participant (Figure 1A). Sessions were separated by at least one week (mean inter-session interval: 28.4 days; SD: 51.2) to prevent carry-over effects of TMS. During the first session, participants completed a short training of the experimental task followed by two runs of a language localizer task and two runs of the experimental task. The second and third session each began with a short practice of the task, after which participants were administered effective or sham iTBS over the pre-SMA. Participants then completed two runs of the experimental task. The TMS laboratory was situated close to the MR unit which enabled us to transfer participants rapidly to the MR scanner after stimulation (mean time end of stimulation until beginning of functional scan: 6.6 min). To avoid any interference of movement with the stimulation effect, participants were transferred in an MR-compatible wheelchair. During functional MRI, all stimuli were presented using the software Presentation (version 18.0, Neurobehavioral Systems, Berkeley, USA, www.neurobs.com). Visual stimuli were back-projected onto a mirror mounted on the head coil. Auditory stimuli were played via MR-compatible in-ear headphones (Sensimetrics, Gloucester, USA, http://www.sens.com/). At the beginning of each fMRI session, participants performed a short volume test in the scanner with one intact passage of the language

localizer and background scanner noise to make sure they could understand the stimuli well.

Language Localizer

The language localizer task was adapted from (Scott et al., 2016). In this task, participants listen to intact and acoustically degraded passages from Alice in Wonderland. Materials for the degraded passages as well as the experimental structure were provided by Evelina Fedorenko (`https://evlab.mit.edu/alice`). The intact passages were taken from the freely available German translation of Alice in Wonderland (`https://www.projekt-gutenberg.org/carroll/alice/alice.html`) and were recorded by a professional native German female speaker in a soundproof room. Recordings were then cut using Praat software (version 6.0.56, `https://www.praat.org`) and normalized using Audacity software (version 2.3.2, `https://www.audacityteam.org/`). In total, 24 intact and 24 acoustically degraded passages were prepared. The language localizer task is constructed as a block design. Each run consists of six intact and six degraded passages interspersed with four fixation periods. Listening passages are each 18 s long and fixation periods 12 s long, thus resulting in a total length of 4.4 min per run and 8.8 min of the whole task. Participants were instructed to lie still and quietly listen to the passages. At the beginning, participants performed a short volume test in the scanner with one intact trial and background scanner noise to make sure that they could hear the stimuli well.

Experimental Paradigm

Two tasks were implemented in the fMRI experiment in a mixed design: a semantic judgment task with varying cognitive demand and a non-verbal control task (Figure 1B). In both tasks, participants were required to decide whether an auditory stimulus matches with a presented image via yes/no-button press using the index and middle finger of their left hand. Since the experiment was planned to be also implemented in people with post-stroke aphasia, the left hand was used in all participants to avoid potential confounds through hemiparesis in the aphasia group. Further, this allowed us to shift motor activity related to the button press to the right hemisphere. The order of buttons was counterbalanced across participants. Tasks were presented in mini-blocks of four trials per task and blocks were separated by rest intervals of 3.75 s (2/3 of all intervals) or 16 s (1/3 of all intervals). Individual trials were 3.5 s long including presentation of the auditory stimulus, the object picture, and button press by the participant. Trials within blocks were interspersed with jittered inter-stimulus intervals between 2.5 and 7 s. Each run included 88 stimuli with 32 items per condition of the semantic judgment task and 24 items of the control task resulting in a total length of 13.8 min per run. Participants completed two runs per session.

Semantic judgment task

The semantic judgment task consisted of a word-picture matching (WPM) and a feature-picture matching (FPM) condition, thus varying with respect to the semantic demand of an item (Figure 1C). During both conditions, participants listened to a short phrase (e.g., "Is a banana" or "Is sour") followed by a picture of an object at the offset of the auditory stimulus. They were then asked to judge if the auditory phrase and the presented object match. Stimuli were chosen from eight categories (four living: birds, fruits, mammals, and vegetables; four non-living: clothes, furniture, tools, and vehicles) according to German norm data for semantic typicality (Schröder et al., 2012). From each category, 12 members were selected, 2/3 of them representing typical and 1/3 representing atypical items of the respective category. Hence, in total, 96 stimuli were developed. For each item, a feature from available concept property norms (Devereux et al., 2014) was chosen so that within every category, items could be paired up with regard to their grammatical gender and their feature. In this way, we made sure that every object was introduced with the appropriate gender through the indefinite article both in the congruent and incongruent condition in the auditory stimulus in the WPM condition ("Is a banana" or "Is a lemon"), thus precluding any syntactic clues on accuracy. In German, the indefinite article can take two forms: feminine "eine" and masculine and neutral "ein". Accordingly, items with male and neutral gender could be paired up together and items with female gender were paired up separately. Further, the arrangement in pairs allowed us to balance the occurrence and to control the semantic value of the features. That is, every feature property was once used as congruent and as incongruent. Since item pairs were within categories, we assured that both congruent and incongruent features were semantically associated with the items. Through this approach, we aimed at avoiding any response bias which could be introduced when an incongruent feature has a bigger semantic distance than the congruent feature from the target item. All auditory stimuli were recorded through the same professional native German female speaker as in the language localizer. Recordings were processed in the same way: They were cut using Praat and normalized via Audacity software.

Across categories, items were balanced for lexical frequency of words and lexical frequency of features using the dlexDB database (Heister et al., 2011). There was no significant difference between frequencies of words (M = 10.27, SD = 23.65) and features (M = 13.63, SD = 23.50), $t(185)$ = 0.98, p = .331). Additionally, items were also balanced across categories for length in phonemes, length in syllables, and length in seconds of the audio files of words and features respectively. In comparison, audio files of words (M = 1.24 s, SD = 0.13) were longer than those of features (M = 1.16 s, SD = 0.18), $t(176)$ = 3.81, p < .001). We dealt with this difference in the length of audio files by designing

the paradigm in a way that pictures of objects only appeared at the offset of each auditory stimulus, thus not depending the decision-making process on the length of the audio files. Pictures for stimulus items were taken from the freely available Bank of Standardized stimuli (Brodeur et al., 2014, 2010) and the colored picture set by Moreno-Martínez and Montoro (2012) or bought through a license of MPI CBS on Shutterstock. Objects were presented on a white background and all pictures were cropped to a size of 720 x 540 pixels. Stimuli of the semantic judgment task were investigated in a pilot experiment (*n* = 50) beforehand to confirm the intended modulation in task demand and to validate name and feature agreement for each item. Stimuli for the final set were only chosen if they showed at least 80% agreement for the word-picture and the feature-picture matching conditions.

We developed six individual stimuli lists per participant (three sessions with two runs each) such that every item appeared once in every condition across runs and sessions. Conditions and congruency were balanced across runs with pairs of congruent and incongruent stimuli never occurring in the same run. Across participants and runs, accuracy and congruency of individual items were pseudorandomized. After balancing procedures, stimuli lists were randomized.

Tone judgment task
The non-verbal control task consisted of sinewave tones at different frequencies (300–825 Hz), which were presented in a sequence of two tones (Figure 1C). Tones in a sequence always had a difference in frequency of 250 Hz. Individual tones were generated using a pure tone generator in Matlab with the following parameters: sampling frequency of 16000 Hz, duration of 450 ms, and fade-in and fade-out duration of 10 ms each. Afterwards, tones were paired up using Audacity software so that each tone once appeared first and once second in a sequence. An inter-tone interval of 300 ms was included in each sequence. Thus, each tone sequence had a length of 1200 ms which equaled the average length of all verbal stimuli. In the control task, participants heard a tone sequence and were asked to match this with a picture of an arrow pointing diagonally upwards or downwards which appeared at the offset of the auditory stimulus. Like in the semantic judgment task, participants had to indicate their choice via button press. Through this process, we aimed at keeping the task as similar as possible to the semantic judgment task but without any verbal processing involved.

Magnetic Resonance Imaging
MRI data were collected at a 3T Siemens Magnetom Skyra scanner (Siemens, Erlangen, Germany) with a 32-channel head coil. For functional scans, a gradient-echo echo-planar imaging multiband sequence (Feinberg et al., 2010) was used with the following parameters: TR: 2000 ms, TE: 22 ms, flip angle: 80°, voxel size:

2.48 x 2.48 x 2.75 mm with a 0.25 mm interslice gap, FOV: 204 mm, multiband acceleration factor: 3, number of slices per volume: 60 axial slices with interleaved order covering the whole brain. For the language localizer task, 266 volumes were acquired. For the experimental task, a total of 842 volumes per session were acquired. For distortion correction, field maps (pepolar images) were obtained at the end of each session (TR: 8000 ms, TE: 50 ms). Additionally, a high-resolution, T1-weighted 3D volume was obtained from the in-house database if available and not older than two years or was acquired after the functional scans on the first session using an MPRAGE sequence (176 slices, whole-brain coverage, TR: 2300 ms, TE: 2.98 ms, voxel size: 1 x 1 x 1 mm, matrix size: 256 x 240 mm, flip angle: 9°).

Intermittent Theta Burst Stimulation
During the second and third session, participants received once effective and once sham rTMS prior to fMRI (Figure 1A). Session order was counterbalanced across participants. rTMS was delivered using the iTBS stimulation protocol which consists of bursts of three pulses at 50 Hz given every 200 ms in two second trains, repeated every ten seconds over 190 seconds for a total of 600 pulses (Huang et al., 2005). We chose to use TBS since its high-frequency protocols have been reported to induce longer lasting after-effects with a duration of up to one hour (Chung et al., 2016). We used stereotactic neuronavigation (TMS Navigator, Localite, Bonn, Germany) based on coregistered individual T1-weighted images to precisely navigate the coil over the target area and maintain its location and orientation throughout the experiment.

iTBS was applied over the pre-SMA. We used an individualized stimulation approach where the stimulation coordinates of each participant were based on activation patterns within a pre-defined ROI for the experimental task during the first session. To this end, fMRI data from the first session were preprocessed using fMRIPrep 20.2.3 and analyzed using SPM12. A ROI mask of the pre-SMA based on a freely available probabilistic cytoarchitectonic map (Ruan et al., 2018) was created, thresholded at greater 0.3, and binarized. Activation in individuals' subject space for the contrast semantic judgment > rest was then inclusively masked using the resampled pre-SMA ROI. Significant clusters were identified after FWE-correction on peak level at $p < 0.05$. The global peak of the strongest cluster within the pre-SMA ROI was identified as the stimulation target in each participant. Figure S1 displays the individual stimulation sites within the mask. Figure S2 shows the location of individual stimulation sites with respect to two cognitive networks of interest: general semantic cognition (Jackson, 2021) and the multiple-demand network (Fedorenko et al., 2013).

iTBS was applied via a MagPro X100 stimulator (MagVenture, Farum, Denmark) equipped with a passively cooled MCFB65 figure-of-eight coil. For sham

stimulation, we used the corresponding placebo coil (MCF-P-B65), which features the same mechanical outline and acoustic noise as the effective coil but provides an effective field reduction of ~80%. During stimulation, the handle of the coil was pointed in a posterior direction (Allen et al., 2018; Taylor et al., 2007; Willacker et al., 2020). Stimulation intensity was set to 90% of individual resting motor threshold (RMT), which was determined during the second session. RMT was defined as the lowest stimulation intensity producing at least five motor evoked potentials of $\geq$ 50 μV in the relaxed first dorsal interosseous muscle when single-pulse TMS was applied to the right motor cortex ten times. The overall application of TMS pulses per sessions was well within safety limits and the whole procedure was in accordance with the current safety guidelines (Rossi et al., 2009).

Data Analyses

Behavioral data

Accuracy and reaction time data of each session were analyzed using mixed-effects models with a logistic regression for accuracy data due to their binary nature and a linear regression for log-transformed reaction time data. We only analyzed reaction times for correct responses. Contrast coding was done via sum coding where the intercept represents the grand mean across conditions and the model coefficients represent the difference between the mean of the respective condition and the grand mean. Based on the research questions of this study, session (i.e., baseline, effective or sham stimulation) and condition (WPM, FPM or tone judgment) along with their interaction term were always entered as fixed effects. Next, we used stepwise model selection to determine the best-fitting model based on the Akaike Information Criterion (AIC), where a model was considered meaningfully more informative if it decreased the AIC by at least two points (Burnham and Anderson, 2004). The AIC reduces overfitting by considering model complexity and simultaneously penalizing models with more parameters. First, the optimal random effects structure was assessed; next, which factors of congruency, stimulation order, age, and task optimized the models; and finally, interaction terms were evaluated. Table S1 displays the model selection procedure for accuracy data. The optimal model included fixed effects for session, condition, congruency, and age as well as a three-way interaction for session, condition, and congruency, and a random intercept for participants (Equation 1). Table S2 displays the model selection procedure for reaction time data. Here, the optimal model included fixed effects for session, condition, congruency, and age, and interactions between condition and congruency and session and condition. As random effects, the model included by-participant random intercepts and by-participant random slopes for session as well as random intercepts for auditory stimuli (Equation 2). P-values were obtained by likelihood ratio tests

of the full model with the effect in question against the model without the effect in question. Statistical models were performed with R (version 4.1.0; Team, 2021) and the packages lme4 (Bates et al., 2015) for mixed models and bblme (Bolker and Team, 2022) for model comparisons. Plots and result tables were generated using the packages sjPlot (Lüdecke, 2021) and ggeffects (Lüdecke, 2018).

$$
\begin{aligned}
Accuracy = \beta_0 &+ \beta_1 Session + \beta_2 Condition+ \\
&\beta_3 Congruency + \beta_4 Age+ \\
&\beta_5 Session \times Condition+ \\
&\beta_6 Session \times Congruency+ \\
&\beta_7 Condition \times Congruency+ \\
&\beta_8 Session \times Condition \times Congruency+ \\
&(1|Subject) + \varepsilon
\end{aligned}
\tag{1}
$$

$$
\begin{aligned}
\log(Reaction\ time) = \beta_0 &+ \beta_1 Session+ \\
\beta_2 Condition + \beta_3 &Congruency + \beta_4 Age+ \\
&\beta_5 Condition \times Congruency+ \\
&\beta_6 Session \times Condition+ \\
&(1 + Session|Subject)+ \\
&(1 + |Auditory\ stimulus) + \varepsilon
\end{aligned}
\tag{2}
$$

Preprocessing of MRI data

Preprocessing of MRI data was performed using fMRIPrep 20.2.3 (Esteban et al., 2019) which is based on Nipype 1.6.1 (Gorgolewski et al., 2011). Preprocessing steps of functional images included slice-time correction, realignment, distortion correction, co-registration of the T1-weighted and functional EPI images, and normalization. Anatomical images were skull-stripped, segmented, and normalized to standard space. Images were normalized to the MNI152NLin6Asym template. A detailed description of the preprocessing steps is included in Supplementary Materials. After preprocessing, functional data were smoothed with an isotropic 5 mm FWHM Gaussian kernel, and analyzed in SPM12 (Wellcome Trust Centre for Neuroimaging) in Matlab (version R2021a; The MathWorks Inc., Natick, MA).

Whole-brain analyses

Functional MRI data were modelled using the two-step procedure. At the first level, data were entered into individual general linear models (GLM) for each session and participant. For the localizer, the GLM included boxcar regressors convolved with the canonical hemodynamic response function (HRF) for the task blocks of the intact and degraded listening passages. Individual thresholded (gray matter probability > 0.2) gray matter masks were used as explicit masks. For the experimental task, regressors for the three conditions and a separate regressor for error trials were included in the GLM.

Individual trials were modelled as stick functions convolved with the canonical HRF. To account for condition- and trial-specific differences in reaction time, the duration of a trial was defined as the length of the auditory stimulus plus the reaction time. For all tasks, models included regressors of no interest: six motion parameters and individual regressors for strong volume-to-volume movement as indicated by values of framewise displacement > 0.7. Further, temporal and spatial derivatives were modelled for each condition, and a high-pass filter (cutoff 128 s) was applied to remove low-frequency noise. Contrast images were generated by estimating contrasts for each condition against rest and direct contrasts between conditions.

For the experimental task, contrast images were then entered intro group-level random effects models. For the first session, one-sample t-tests were computed to define group activations for the different conditions. To assess differences in activation between effective and sham iTBS, contrast images from the sham session were subtracted from contrast images from the effective session, and the difference images were then submitted to random effects models and session effects were estimated using one-sample t-tests. For all second-level analyses, a gray matter mask was applied, which restricted statistical tests to voxels with a gray matter probability > 0.3 (SPM12 tissue probability map). Results were thresholded at $p < 0.05$ at peak level and corrected at cluster level for the family-wise error (FWE) rate at $p < 0.05$. Anatomical locations were identified with the Harvard-Oxford cortical structural atlases distributed with FSL (`https://fsl.fmrib.ox.ac.uk`).

To assess the relationship between differences in activation and differences in behavior due to iTBS, we extracted PSC for our a-priori defined stimulation site of pre-SMA and for clusters showing a significant effect of stimulation ($n = 6$; see Table 1) using the MarsBar toolbox (version 0.45; Brett et al., 2002). For the pre-SMA, PSC was extracted for a cluster centered at each individual stimulation site and containing the 10% strongest activated voxels for the contrast semantic judgment > rest, which was identical to the contrast used for the definition of the stimulation site. Data were then entered into correlation analyses where the difference in PSC for a certain condition was correlated with the difference in accuracy and reaction time between effective and sham sessions.

Analysis of subject-specific functional regions of interest

Data from the language localizer task were analyzed employing the group-constrained subject-specific approach (Julian et al., 2012). This method allows the identification of individual functional regions of interest (fROIs) sensitive to language processing (Fedorenko et al., 2010), which were then used to characterize response profiles in the independent data set of the experimental task. The definition of fROIs followed the procedure described by (Fedorenko et al., 2010) and

was done using the spm_ss toolbox (Nieto-Castañón and Fedorenko, 2012): First, individual activation maps for our contrast of interest of the localizer task (intact > acoustically degraded speech) were thresholded at a voxel-wise false discovery rate (FDR) of q < 0.05 at whole-brain level (Genovese et al., 2002) and then overlaid on top of each other. The resulting probabilistic overlap map displayed how many participants showed activation at each voxel. Next, the overlap map was smoothed (5 mm), thresholded at 3 participants (10%; cf. Fedorenko et al., 2010), and parcellated using a watershed algorithm (Meyer, 1991). The watershed algorithm resulted in 37 fROIs. Third, only those ROIs from the parcellation were retained where at least 60% of participants had any supra-threshold voxels (cf. Fedorenko et al., 2010; Julian et al., 2012). This led to a final sample of 25 parcels (Figure S3). To confirm that these parcels were indeed relevant to language processing, independent of the task, we entered them in a random-effects group-level analysis using the experimental task data. Results were calculated for the contrast language (i.e., WPM + FPM) > rest and FDR-corrected at q < 0.05. Results showed that all 25 parcels were significantly stronger activated for the language task (Table S3). Finally, subject-specific fROIs were defined as the 10% most active voxels in each participant for the localizer contrast intact > degraded speech within each parcel. Since we were interested in the potential effect of iTBS on differences in activation in the language-specific fROIs, we extracted PSC for each fROI and condition for the experimental task using the MarsBar toolbox (version 0.45; Brett et al., 2002). The data were then entered into a linear model with predictors for stimulation type (effective or sham) and fROI and their interaction term. Post-hoc comparisons were applied using the package emmeans (Lenth, 2020).

Functional connectivity analysis

We were interested in potential changes in functional connectivity induced by iTBS. To this end, we conducted psychophysiological interaction (PPI) analyses using the gPPI toolbox (McLaren et al., 2012). Seed regions were defined for significant global cluster peaks for the contrast of effective and sham session (n = 6, cf. Table 1) and for our stimulation site, bilateral pre-SMA. Binary, resampled masks were created for each seed by building a spherical ROI with a radius of 10 mm in MarsBar. Next, for each participant, individual ROIs were created by extracting the 10% most active voxels in each seed mask of a given contrast image. For the seed masks of pre-SMA, we used the contrast semantic judgment task (i.e., WPM + FPM) > rest, which was the same contrast used to define individual stimulation coordinates.

For the gPPI, individual regression models were set up for each ROI and session containing the deconvolved time series of the first eigenvariate of the BOLD signal from the respective ROI as the physiological vari-

able, regressors for the three task conditions and errors as the psychological variable, and the interaction of both variables as the PPI term. Models were adjusted for an omnibus F-test of all task regressors. Subsequently, first-level GLMs were calculated. We were specifically interested in potential differences between effective and sham iTBS sessions for the contrast semantic judgment > tone judgment. To this end, contrast images from the sham session were subtracted from contrast images from the effective session and the difference images were submitted to random-effects models for group analysis. Significant clusters were determined via one-sample t-tests. A gray matter mask was applied as described for the univariate analyses. Results were thresholded at p <0.01 at peak level and FWE-corrected p <0.05 at cluster level.

We also explored a relationship between stimulation-induced changes in functional connectivity and behavior. To this end, we extracted pre-SMA-to-ROI PPI connectivity for effective and sham sessions for the contrast semantic judgment > tone judgment where ROI refers to the six seed regions described above. We then correlated the difference between effective and sham connectivity for each pre-SMA-ROI pair with the difference between effective and sham in accuracy and reaction time.

Data Availability

All behavioral data as well as extracted beta weights generated or analyzed during this study have been deposited in a public repository on Gitlab `https://gitlab.gwdg.de/mdn-in-aging-and-aphasia/mdn_aph`. This repository also holds all self-written analysis code used for this project. Unthresholded statistical group maps for fMRI and gPPI results are made publicly available on NeuroVault: `https://neurovault.org/collections/13064/`.
Raw and single subject neuroimaging data are protected under the General Data Protection Regulation (EU) and can only be made available from the authors upon reasonable request.

Conflict of Interest

The authors declare that no competing interests exist.

Acknowledgments

Bibliography

Abel, S., Dressel, K., Weiller, C., and Huber, W. Enhancement and suppression in a lexical interference fMRI-paradigm. *Brain and Behavior*, 2(2):109–127, Mar. 2012. doi: 10.1002/brb3.31.

Abel, S., Weiller, C., Huber, W., Willmes, K., and Specht, K. Therapy-induced brain reorganization patterns in aphasia. *Brain*, 138(4):1097–1112, Apr. 2015. doi: 10.1093/brain/awv022.

Abellaneda-Pérez, K., Vaqué-Alcázar, L., Solé-Padullés, C., and Bartrés-Faz, D. Combining non-invasive brain stimulation with functional magnetic resonance imaging to investigate the neural substrates of cognitive aging. *Journal of Neuroscience Research*, 100(5):1159–1170, 2022. doi: 10.1002/jnr.24514.

Allen, C., Singh, K. D., Verbruggen, F., and Chambers, C. D. Evidence for parallel activation of the pre-supplementary motor area and inferior frontal cortex during response inhibition: A combined MEG and TMS study. *Royal Society Open Science*, 5(2):171369, Feb. 2018. doi: 10.1098/rsos.171369.

Amedi, A., Floel, A., Knecht, S., Zohary, E., and Cohen, L. G. Transcranial magnetic stimulation of the occipital pole interferes with verbal processing in blind subjects. *Nature Neuroscience*, 7(11):1266–1270, Nov. 2004. doi: 10.1038/nn1328.

Antonenko, D., Thams, F., Grittner, U., Uhrich, J., Glöckner, F., Li, S.-C., and Flöel, A. Randomized trial of cognitive training and brain stimulation in non-demented older adults. *Alzheimer's & Dementia (New York, N. Y.)*, 8(1):e12262, 2022. doi: 10.1002/trc2.12262.

Badre, D., Poldrack, R. A., Paré-Blagoev, E. J., Insler, R. Z., and Wagner, A. D. Dissociable Controlled Retrieval and Generalized Selection Mechanisms in Ventrolateral Prefrontal Cortex. *Neuron*, 47(6):907–918, Sept. 2005. doi: 10.1016/j.neuron.2005.07.023.

Bates, D., Mächler, M., Bolker, B., and Walker, S. Fitting linear mixed-effects models using lme4. *Journal of Statistical Software*, 67(1):1–48, 2015. doi: 10.18637/jss.v067.i01.

Binder, J. R., Desai, R. H., Graves, W. W., and Conant, L. L. Where Is the Semantic System? A Critical Review and Meta-Analysis of 120 Functional Neuroimaging Studies. *Cerebral Cortex*, 19(12):2767–2796, Dec. 2009. doi: 10.1093/cercor/bhp055.

Blankenburg, F., Ruff, C. C., Bestmann, S., Bjoertomt, O., Josephs, O., Deichmann, R., and Driver, J. Studying the Role of Human Parietal Cortex in Visuospatial Attention with Concurrent TMS–fMRI. *Cerebral Cortex*, 20(11):2702–2711, Nov. 2010. doi: 10.1093/cercor/bhq015.

Bolker, B. and Team, R. C. Bbmle: Tools for General Maximum Likelihood Estimation, 2022.

Booth, S. J., Taylor, J. R., Brown, L. J. E., and Pobric, G. The effects of transcranial alternating current stimulation on memory performance in healthy adults: A systematic review. *Cortex*, 147:112–139, Feb. 2022. doi: 10.1016/j.cortex.2021.12.001.

Brett, M., Anton, J.-L., Valabregue, R., and Poline, J.-B. Region of Interest Analysis Using an SPM Toolbox. *Neuroimage*, 16, Jan. 2002. doi: 10.1016/S1053-8119(02)90013-3.

Brodeur, M. B., Dionne-Dostie, E., Montreuil, T., and Lepage, M. The Bank of Standardized Stimuli (BOSS), a New Set of 480 Normative Photos of Objects to Be Used as Visual Stimuli in Cognitive Research. *PLOS ONE*, 5(5):e10773, May 2010. doi: 10.1371/journal.pone.0010773.

Brodeur, M. B., Guérard, K., and Bouras, M. Bank of Standardized Stimuli (BOSS) Phase II: 930 New Normative Photos. *PLOS ONE*, 9(9):e106953, Sept. 2014. doi: 10.1371/journal.pone.0106953.

Burke, D. M. and Shafto, M. A. Aging and Language Production. *Current directions in psychological science*, 13(1):21, 2004. doi: 10.1111/j.0963-7214.2004.01301006.x.

Burnham, K. P. and Anderson, D. R. Multimodel Inference: Understanding AIC and BIC in Model Selection. *Sociological Methods & Research*, 33(2):261–304, Nov. 2004. doi: 10.1177/0049124104268644.

Cabeza, R., Albert, M., Belleville, S., Craik, F. I. M., Duarte, A., Grady, C. L., Lindenberger, U., Nyberg, L., Park, D. C., Reuter-Lorenz, P. A., Rugg, M. D., Steffener, J., and Rajah, M. N. Maintenance, reserve and compensation: The cognitive neuroscience of healthy ageing. *Nature Reviews Neuroscience*, 19(11):701–710, Nov. 2018. doi: 10.1038/s41583-018-0068-2.

Camilleri, J., Müller, V., Fox, P., Laird, A., Hoffstaedter, F., Kalenscher, T., and Eickhoff, S. Definition and characterization of an extended multiple-demand network. *NeuroImage*, 165:138–147, Jan. 2018. doi: 10.1016/j.neuroimage.2017.10.020.

Cárdenas-Morales, L., Grön, G., and Kammer, T. Exploring the after-effects of theta burst magnetic stimulation on the human motor cortex: A functional imaging study. *Human Brain Mapping*, 32(11):1948–1960, Nov. 2011. doi: 10.1002/hbm.21160.

Chiou, R., Humphreys, G. F., Jung, J., and Lambon Ralph, M. A. Controlled semantic cognition relies upon dynamic and flexible interactions between the executive 'semantic control' and hub-and-spoke 'semantic representation' systems. *Cortex*, 103:100–116, June 2018. doi: 10.1016/j.cortex.2018.02.018.

Chung, S. W., Hill, A. T., Rogasch, N. C., Hoy, K. E., and Fitzgerald, P. B. Use of theta-burst stimulation in changing excitability of motor cortex: A systematic review and meta-analysis. *Neuroscience & Biobehavioral Reviews*, 63:43–64, Apr. 2016. doi: 10.1016/j.neubiorev.2016.01.008.

Cristescu, T. C., Devlin, J. T., and Nobre, A. C. Orienting attention to semantic categories. *NeuroImage*, 33(4):1178–1187, Dec. 2006. doi: 10.1016/j.neuroimage.2006.08.017.

Debarnot, U., Crépon, B., Orriols, E., Abram, M., Charron, S., Lion, S., Roca, P., Oppenheim, C., Gueguen, B., Ergis, A.-M., Baron, J.-C., and Piolino, P. Intermittent theta burst stimulation over left BA10 enhances virtual reality-based prospective memory in healthy aged subjects. *Neurobiology of Aging*, 36(8):2360–2369, Aug. 2015. doi: 10.1016/j.neurobiolaging.2015.05.001.

DeDe, G. and Knilans, J. Language comprehension in aging. In Wright, H. H., editor, *Cognition, Language and Aging*, pages 107–133. John Benjamins Publishing Company, Amsterdam, Mar. 2016. ISBN 978-90-272-1232-0 978-90-272-6731-3. doi: 10.1075/z.200.05ded.

Dehaene, S. and Cohen, L. The unique role of the visual word form area in reading. *Trends in Cognitive Sciences*, 15(6):254–262, June 2011. doi: 10.1016/j.tics.2011.04.003.

Demeter, E. Enhancing Cognition with Theta Burst Stimulation. *Current Behavioral Neuroscience Reports*, 3(2):87–94, June 2016. doi: 10.1007/s40473-016-0072-7.

Devereux, B. J., Tyler, L. K., Geertzen, J., and Randall, B. The Centre for Speech, Language and the Brain (CSLB) concept property norms. *Behavior Research Methods*, 46(4):1119–1127, Dec. 2014. doi: 10.3758/s13428-013-0420-4.

Duncan, J. The multiple-demand (MD) system of the primate brain: Mental programs for intelligent behaviour. *Trends in Cognitive Sciences*, 14(4):172–179, Apr. 2010. doi: 10.1016/j.tics.2010.01.004.

Esteban, O., Markiewicz, C. J., Blair, R. W., Moodie, C. A., Isik, A. I., Erramuzpe, A., Kent, J. D., Goncalves, M., DuPre, E., Snyder, M., Oya, H., Ghosh, S. S., Wright, J., Durnez, J., Poldrack, R. A., and Gorgolewski, K. J. fMRIPrep: A robust preprocessing pipeline for functional MRI. *Nature Methods*, 16(1):111–116, Jan. 2019. doi: 10.1038/s41592-018-0235-4.

Fedorenko, E., Hsieh, P.-J., Nieto-Castañón, A., Whitfield-Gabrieli, S., and Kanwisher, N. New Method for fMRI Investigations of Language: Defining ROIs Functionally in Individual Subjects. *Journal of Neurophysiology*, 104(2):1177–1194, Apr. 2010. doi: 10.1152/jn.00032.2010.

Fedorenko, E., Duncan, J., and Kanwisher, N. Broad domain generality in focal regions of frontal and parietal cortex. *Proceedings of the National Academy of Sciences*, 110(41):16616–16621, Oct. 2013. doi: 10.1073/pnas.1315235110.

Feinberg, D. A., Moeller, S., Smith, S. M., Auerbach, E., Ramanna, S., Glasser, M. F., Miller, K. L., Ugurbil, K., and Yacoub, E. Multiplexed Echo Planar Imaging for Sub-Second Whole Brain FMRI and Fast Diffusion Imaging. *PLOS ONE*, 5(12):e15710, Dec. 2010. doi: 10.1371/journal.pone.0015710.

Feredoes, E., Heinen, K., Weiskopf, N., Ruff, C., and Driver, J. Causal evidence for frontal involvement in memory target maintenance by posterior brain areas during distracter interference of visual working memory. *Proceedings of the National Academy of Sciences*, 108(42):17510–17515, Oct. 2011. doi: 10.1073/pnas.1106439108.

Forseth, K. J., Kadipasaoglu, C. M., Conner, C. R., Hickok, G., Knight, R. T., and Tandon, N. A lexical semantic hub for heteromodal naming in middle fusiform gyrus. *Brain*, 141(7):2112–2126, July 2018. doi: 10.1093/brain/awy120.

Genovese, C. R., Lazar, N. A., and Nichols, T. Thresholding of Statistical Maps in Functional Neuroimaging Using the False Discovery Rate. *NeuroImage*, 15(4):870–878, Apr. 2002. doi: 10.1006/nimg.2001.1037.

Geranmayeh, F., Wise, R. J. S., Mehta, A., and Leech, R. Overlapping Networks Engaged during Spoken Language Production and Its Cognitive Control. *Journal of Neuroscience*, 34(26):8728–8740, June 2014. doi: 10.1523/JNEUROSCI.0428-14.2014.

Goldthorpe, R. A., Rapley, J. M., and Violante, I. R. A Systematic Review of Non-invasive Brain Stimulation Applications to Memory in Healthy Aging. *Frontiers in Neurology*, 11, 2020.

Goral, M., Clark-Cotton, M., Spiro, A., Obler, L. K., Verkuilen, J., and Albert, M. L. The Contribution of Set Switching and Working Memory to Sentence Processing in Older Adults. *Experimental aging research*, 37(5):516–538, Oct. 2011. doi: 10.1080/0361073X.2011.619858.

Gorgolewski, K., Burns, C., Madison, C., Clark, D., Halchenko, Y., Waskom, M., and Ghosh, S. Nipype: A Flexible, Lightweight and Extensible Neuroimaging Data Processing Framework in Python. *Frontiers in Neuroinformatics*, 5:13, 2011. doi: 10.3389/fninf.2011.00013.

Grady, C. L. The cognitive neuroscience of ageing. *Nature Reviews Neuroscience*, 13(7):491–505, July 2012. doi: 10.1038/nrn3256.

Grill-Spector, K. The neural basis of object perception. *Current Opinion in Neurobiology*, 13(2):159–166, Apr. 2003. doi: 10.1016/S0959-4388(03)00040-0.

Halko, M. A., Farzan, F., Eldaief, M. C., Schmahmann, J. D., and Pascual-Leone, A. Intermittent Theta-Burst Stimulation of the Lateral Cerebellum Increases Functional Connectivity of the Default Network. *The Journal of Neuroscience*, 34(36):12049–12056, Sept. 2014. doi: 10.1523/JNEUROSCI.1776-14.2014.

Hartwigsen, G. and Volz, L. J. Probing rapid network reorganization of motor and language functions via neuromodulation and neuroimaging. *NeuroImage*, 224:117449, Jan. 2021. doi: 10.1016/j.neuroimage.2020.117449.

Hartwigsen, G., Bzdok, D., Klein, M., Wawrzyniak, M., Stockert, A., Wrede, K., Classen, J., and Saur, D. Rapid short-term reorganization in the language network. *eLife*, 6, 2017. doi: 10.7554/eLife.25964.001.

Hartwigsen, G. The neurophysiology of language: Insights from non-invasive brain stimulation in the healthy human brain. *Brain and Language*, 148:81–94, Sept. 2015. doi: 10.1016/j.bandl.2014.10.007.

Hartwigsen, G. Flexible Redistribution in Cognitive Networks. *Trends in Cognitive Sciences*, 22(8):687–698, Aug. 2018. doi: 10.1016/j.tics.2018.05.008.

Heath, S., McMahon, K. L., Nickels, L., Angwin, A., MacDonald, A. D., van Hees, S., Johnson, K., McKinnon, E., and Copland, D. A. Neural mechanisms underlying the facilitation of naming in aphasia using a semantic task: An fMRI study. *BMC Neuroscience*, 13(1):98, Aug. 2012. doi: 10.1186/1471-2202-13-98.

Hedden, T. and Gabrieli, J. D. E. Insights into the ageing mind: A view from cognitive neuroscience. *Nature Reviews Neuroscience*, 5(2):87–96, Feb. 2004. doi: 10.1038/nrn1323.

Heister, J., Würzner, K.-M., Bubenzer, J., Pohl, E., Hanneforth, T., Geyken, A., and Kliegl, R. dlexDB – eine lexikalische Datenbank für die psychologische und linguistische Forschung. *Psychologische Rundschau*, 62(1):10–20, Jan. 2011. doi: 10.1026/0033-3042/a000029.

Henderson, A. and Wright, H. H. Cognition, language, and aging: An introduction. In Wright, H. H., editor, *Cognition, Language and Aging*, pages 1–11. John Benjamins Publishing Company, Amsterdam, Mar. 2016. ISBN 978-90-272-1232-0 978-90-272-6731-3. doi: 10.1075/z.200.01hen.

Hermiller, M. S., Dave, S., Wert, S. L., VanHaerents, S., Riley, M., Weintraub, S., Mesulam, M. M., and Voss, J. L. Evidence from theta-burst stimulation that age-related de-differentiation of the hippocampal network is functional for episodic memory. *Neurobiology of Aging*, 109:145–157, Jan. 2022. doi: 10.1016/j.neurobiolaging.2021.09.018.

Hoffman, P. and Morcom, A. M. Age-related changes in the neural networks supporting semantic cognition: A meta-analysis of 47 functional neuroimaging studies. *Neuroscience & Biobehavioral Reviews*, 84:134–150, Jan. 2018. doi: 10.1016/j.neubiorev.2017.11.010.

Hoffman, P. An individual differences approach to semantic cognition: Divergent effects of age on representation, retrieval and selection. *Scientific Reports*, 8(1):8145, May 2018. doi: 10.1038/s41598-018-26569-0.

Holland, R., Leff, A. P., Josephs, O., Galea, J. M., Desikan, M., Price, C. J., Rothwell, J. C., and Crinion, J. Speech Facilitation by Left Inferior Frontal Cortex Stimulation. *Current Biology*, 21(16):1403–1407, Aug. 2011. doi: 10.1016/j.cub.2011.07.021.

Holland, R., Leff, A. P., Penny, W. D., Rothwell, J. C., and Crinion, J. Modulation of frontal effective connectivity during speech. *Neuroimage*, 140:126–133, Oct. 2016. doi: 10.1016/j.neuroimage.2016.01.037.

Horner, A. J. and Henson, R. N. Priming, response learning and repetition suppression. *Neuropsychologia*, 46(7):1979–1991, June 2008. doi: 10.1016/j.neuropsychologia.2008.01.018.

Hsu, W.-Y., Ku, Y., Zanto, T. P., and Gazzaley, A. Effects of noninvasive brain stimulation on cognitive function in healthy aging and Alzheimer's disease: A systematic review and meta-analysis. *Neurobiology of Aging*, 36(8):2348–2359, Aug. 2015. doi: 10.1016/j.neurobiolaging.2015.04.016.

Huang, Y.-Z., Edwards, M. J., Rounis, E., Bhatia, K. P., and Rothwell, J. C. Theta Burst Stimulation of the Human Motor Cortex. *Neuron*, 45(2):201–206, Jan. 2005. doi: 10.1016/j.neuron.2004.12.033.

Jackson, R. L. The neural correlates of semantic control revisited. *NeuroImage*, 224:117444, Jan. 2021. doi: 10.1016/j.neuroimage.2020.117444.

Julian, J. B., Fedorenko, E., Webster, J., and Kanwisher, N. An algorithmic method for functionally defining regions of interest in the ventral visual pathway. *NeuroImage*, 60(4):2357–2364, May 2012. doi: 10.1016/j.neuroimage.2012.02.055.

Kanwisher, N., McDermott, J., and Chun, M. M. The Fusiform Face Area: A Module in Human Extrastriate Cortex Specialized for Face Perception. *Journal of Neuroscience*, 17(11):4302–4311, June 1997. doi: 10.1523/JNEUROSCI.17-11-04302.1997.

Kemper, S., Crow, A., and Kemtes, K. Eye-Fixation Patterns of High- and Low-Span Young and Older Adults: Down the Garden Path and Back Again. *Psychology and Aging*, 19(1):157–170, 2004. doi: 10.1037/0882-7974.19.1.157.

Kim, K. K., Karunanayaka, P., Privitera, M. D., Holland, S. K., and Szaflarski, J. P. Semantic association investigated with functional MRI and independent component analysis. *Epilepsy & Behavior*, 20(4):613–622, Apr. 2011. doi: 10.1016/j.yebeh.2010.11.010.

Lambon Ralph, M. A., Jefferies, E., Patterson, K., and Rogers, T. T. The neural and computational bases of semantic cognition. *Nature Reviews Neuroscience*, 18(1):42–55, Jan. 2017. doi: 10.1038/nrn.2016.150.

Legon, W., Punzell, S., Dowlati, E., Adams, S. E., Stiles, A. B., and Moran, R. J. Altered Prefrontal Excitation/Inhibition Balance and Prefrontal Output: Markers of Aging in Human Memory Networks. *Cerebral Cortex (New York, N.Y.: 1991)*, 26(11):4315–4326, Oct. 2016. doi: 10.1093/cercor/bhv200.

Lenth, R. Emmeans: Estimated Marginal Means, aka Least-Squares Means. R package version 1.4.8., 2020.

Lüdecke, D. Ggeffects: Tidy Data Frames of Marginal Effects from Regression Models. *Journal of Open Source Software*, 3(26):772, June 2018. doi: 10.21105/joss.00772.

Lüdecke, D. sjPlot - Data Visualization for Statistics in Social Science. Zenodo, 2021.

Mahon, B. Z. and Caramazza, A. Judging semantic similarity: An event-related fMRI study with auditory word stimuli. *Neuroscience*, 169(1):279–286, Aug. 2010. doi: 10.1016/j.neuroscience.2010.04.029.

Martin, S., Williams, K. A., Saur, D., and Hartwigsen, G. Age-related reorganization of functional network architecture in semantic cognition. *Cerebral Cortex*, page bhac387, Oct. 2022. doi: 10.1093/cercor/bhac387.

Martin, S., Saur, D., and Hartwigsen, G. Age-Dependent Contribution of Domain-General Networks to Semantic Cognition. *Cerebral Cortex*, 32(4):870–890, Feb. 2022. doi: 10.1093/cercor/bhab252.

McLaren, D. G., Ries, M. L., Xu, G., and Johnson, S. C. A Generalized Form of Context-Dependent Psychophysiological Interactions (gPPI): A Comparison to Standard Approaches. *Neuroimage*, 61(4):1277–1286, July 2012. doi: 10.1016/j.neuroimage.2012.03.068.

Meinzer, M., Lindenberg, R., Antonenko, D., Flaisch, T., and Floel, A. Anodal Transcranial Direct Current Stimulation Temporarily Reverses Age-Associated Cognitive Decline and Functional Brain Activity Changes. *Journal of Neuroscience*, 33(30):12470–12478, July 2013. doi: 10.1523/JNEUROSCI.5743-12.2013.

Meinzer, M., Lindenberg, R., Sieg, M. M., Nachtigall, L., Ulm, L., and Flöel, A. Transcranial direct current stimulation of the primary motor cortex improves word-retrieval in older adults. *Frontiers in Aging Neuroscience*, 6, 2014.

Meyer, F. Un algorithme optimal pour la ligne de partage des eaux. Dans 8e congrès de reconnaissance des formes et intelligence artificielle. In *8 Me Congrès de Reconnaissance Des Formes et Intelligence Artificielle*, 2, pages 847–857, Lyon, France, 1991.

Mion, M., Patterson, K., Acosta-Cabronero, J., Pengas, G., Izquierdo-Garcia, D., Hong, Y. T., Fryer, T. D., Williams, G. B., Hodges, J. R., and Nestor, P. J. What the left and right anterior fusiform gyri tell us about semantic memory. *Brain: A Journal of Neurology*, 133(11):3256–3268, Nov. 2010. doi: 10.1093/brain/awq272.

Moreno-Martínez, F. J. and Montoro, P. R. An Ecological Alternative to Snodgrass & Vanderwart: 360 High Quality Colour Images with Norms for Seven Psycholinguistic Variables. *PLoS ONE*, 7(5):e37527, May 2012. doi: 10.1371/journal.pone.0037527.

Nagel, I. E., Schumacher, E. H., Goebel, R., and D'Esposito, M. Functional MRI investigation

of verbal selection mechanisms in lateral prefrontal cortex. *NeuroImage*, 43(4):801–807, Dec. 2008. doi: 10.1016/j.neuroimage.2008.07.017.

Nieto-Castañón, A. and Fedorenko, E. Subject-specific functional localizers increase sensitivity and functional resolution of multi-subject analyses. *NeuroImage*, 63(3):1646–1669, Nov. 2012. doi: 10.1016/j.neuroimage.2012.06.065.

Noonan, K. A., Jefferies, E., Visser, M., and Lambon Ralph, M. A. Going beyond Inferior Prefrontal Involvement in Semantic Control: Evidence for the Additional Contribution of Dorsal Angular Gyrus and Posterior Middle Temporal Cortex. *Journal of Cognitive Neuroscience*, 25(11):1824–1850, July 2013. doi: 10.1162/jocn_a_00442.

Obler, L. K., Fein, D., Nicholas, M., and Albert, M. L. Auditory comprehension and aging: Decline in syntactic processing. *Applied Psycholinguistics*, 12(4):433–452, 1991. doi: 10.1017/S0142716400005865.

Palejwala, A. H., Dadario, N. B., Young, I. M., O'Connor, K., Briggs, R. G., Conner, A. K., O'Donoghue, D. L., and Sughrue, M. E. Anatomy and White Matter Connections of the Lingual Gyrus and Cuneus. *World Neurosurgery*, 151:e426–e437, July 2021. doi: 10.1016/j.wneu.2021.04.050.

Park, D. C., Polk, T. A., Park, R., Minear, M., Savage, A., Smith, M. R., and Smith, E. E. Aging Reduces Neural Specialization in Ventral Visual Cortex. *Proceedings of the National Academy of Sciences of the United States of America*, 101(35):13091–13095, 2004. doi: 10.1073/pnas.0405148101.

Richter, M., Miltner, W. H. R., and Straube, T. Association between therapy outcome and right-hemispheric activation in chronic aphasia. *Brain*, 131(5):1391–1401, May 2008. doi: 10.1093/brain/awn043.

Rossi, S., Hallett, M., Rossini, P. M., and Pascual-Leone, A. Safety, ethical considerations, and application guidelines for the use of transcranial magnetic stimulation in clinical practice and research. *Clinical Neurophysiology*, 120(12):2008–2039, Dec. 2009. doi: 10.1016/j.clinph.2009.08.016.

Ruan, J., Bludau, S., Palomero-Gallagher, N., Caspers, S., Mohlberg, H., Eickhoff, S. B., Seitz, R. J., and Amunts, K. Cytoarchitecture, probability maps, and functions of the human supplementary and pre-supplementary motor areas. *Brain Structure and Function*, 223(9):4169–4186, Dec. 2018. doi: 10.1007/s00429-018-1738-6.

Schröder, A., Gemballa, T., Ruppin, S., and Wartenburger, I. German norms for semantic typicality, age of acquisition, and concept familiarity. *Behavior Research Methods*, 44(2): 380–394, June 2012. doi: 10.3758/s13428-011-0164-y.

Scott, T. L., Gallée, J., and Fedorenko, E. A new fun and robust version of an fMRI localizer for the frontotemporal language system. *Cognitive Neuroscience*, 8(3):167–176, 2016. doi: 10.1080/17588928.2016.1201466.

Siebner, H. R., Hartwigsen, G., Kassuba, T., and Rothwell, J. C. How does transcranial magnetic stimulation modify neuronal activity in the brain? Implications for studies of cognition. *Cortex*, 45(9):1035–1042, Oct. 2009. doi: 10.1016/j.cortex.2009.02.007.

Singh, A., Erwin-Grabner, T., Sutcliffe, G., Paulus, W., Dechent, P., Antal, A., and Goya-Maldonado, R. Default mode network alterations after intermittent theta burst stimulation in healthy subjects. *Translational Psychiatry*, 10(1):1–10, Feb. 2020. doi: 10.1038/s41398-020-0754-5.

Sliwinska, M. W., Violante, I. R., Wise, R. J. S., Leech, R., Devlin, J. T., Geranmayeh, F., and Hampshire, A. Stimulating Multiple-Demand Cortex Enhances Vocabulary Learning. *Journal of Neuroscience*, 37(32):7606–7618, Aug. 2017. doi: 10.1523/JNEUROSCI.3857-16.2017.

Spreng, R. N., Wojtowicz, M., and Grady, C. L. Reliable differences in brain activity between young and old adults: A quantitative meta-analysis across multiple cognitive domains. *Neuroscience & Biobehavioral Reviews*, 34(8):1178–1194, July 2010. doi: 10.1016/j.neubiorev.2010.01.009.

Taylor, P. C. J., Nobre, A. C., and Rushworth, M. F. S. Subsecond Changes in Top–Down Control Exerted by Human Medial Frontal Cortex during Conflict and Action Selection: A Combined Transcranial Magnetic Stimulation–Electroencephalography Study. *Journal of Neuroscience*, 27(42):11343–11353, Oct. 2007. doi: 10.1523/JNEUROSCI.2877-07.2007.

Team, R. C. R: A language and environment for statistical computing. R Foundation for Statistical Computing, 2021.

Verhaeghen, P. Aging and vocabulary scores: A meta-analysis. *Psychology and Aging*, 18 (2):332–339, June 2003. doi: 10.1037/0882-7974.18.2.332.

Vidal-Piñeiro, D., Martin-Trias, P., Arenaza-Urquijo, E. M., Sala-Llonch, R., Clemente, I. C., Mena-Sánchez, I., Bargalló, N., Falcón, C., Pascual-Leone, Á., and Bartrés-Faz, D. Task-dependent Activity and Connectivity Predict Episodic Memory Network-based Responses to Brain Stimulation in Healthy Aging. *Brain Stimulation*, 7(2):287–296, Mar. 2014. doi: 10.1016/j.brs.2013.12.016.

Willacker, L., Roccato, M., Can, B. N., Dieterich, M., and Taylor, P. C. J. Reducing variability of perceptual decision making with offline theta-burst TMS of dorsal medial frontal cortex. *Brain Stimulation*, 13(6):1689–1696, Nov. 2020. doi: 10.1016/j.brs.2020.09.011.

Yeo, B. T., Krienen, F. M., Sepulcre, J., Sabuncu, M. R., Lashkari, D., Hollinshead, M., Roffman, J. L., Smoller, J. W., Zöllei, L., Polimeni, J. R., Fischl, B., Liu, H., and Buckner, R. L. The organization of the human cerebral cortex estimated by intrinsic functional connectivity. *Journal of Neurophysiology*, 106(3):1125–1165, Sept. 2011. doi: 10.1152/jn.00338.2011.